

HIGH PERFORMANCE Ir-Re COMPOSITE

Dr. Shanjin He

Ceramic Composites Incorporated
1110 Benfield Blvd, Suites Q-R
Millersville, MD 21108

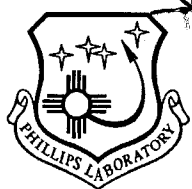
May 1996

Final Report

Distribution authorized to DoD components only; Proprietary Information; May 1996. Other requests for this document shall be referred to AFMC/STI.

WARNING - This document contains technical data whose export is restricted by the Arms Export Control Act (Title 22, U.S.C., Sec 2751 et seq.) or The Export Administration Act of 1979, as amended (Title 50, U.S.C., App. 2401, et seq.). Violations of these export laws are subject to severe criminal penalties. Disseminate IAW the provisions of DoD Directive 5230.25 and AFI 61-204.

DESTRUCTION NOTICE - For classified documents, follow the procedures in DoD 5200.22-M, Industrial Security Manual, Section II-19 or DoD 5200.1-R, Information Security Program Regulation, Chapter IX. For unclassified, limited documents, destroy by any method that will prevent disclosure of contents or reconstruction of the document.



PHILLIPS LABORATORY
Space and Missiles Technology Directorate
AIR FORCE MATERIEL COMMAND
KIRTLAND AIR FORCE BASE, NM 87117-5776

19960715 018

UNCLASSIFIED



AD NUMBER

AD- B212 769

NEW LIMITATION CHANGE

TO

DISTRIBUTION STATEMENT A -
Approved for public release; Distri-
bution unlimited.

Limitation Code: 1

FROM

DISTRIBUTION STATEMENT -

Limitation Code:

AUTHORITY

Janet E. Mosher; Phillips Lab/CA, Kirtland AFB,
N.M.

THIS PAGE IS UNCLASSIFIED

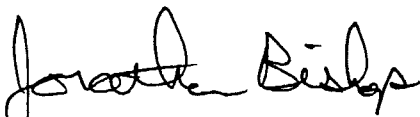
Using Government drawings, specifications, or other data included in this document for any purpose other than Government procurement does not in any way obligate the U.S. Government. The fact that the Government formulated or supplied the drawings, specifications, or other data, does not license the holder or any other person or corporation; or convey any rights or permission to manufacture, use, or sell any patented invention that may relate to them.

This report contains proprietary information and shall not be either released outside the government, or used, duplicated or disclosed in whole or in part for manufacture or procurement, without the written permission of the contractor. This legend shall be marked on any reproduction hereof in whole or in part.

If you change your address, wish to be removed from this mailing list, or your organization no longer employs the addressee, please notify PL/VTs, 3550 Aberdeen Ave SE, Kirtland AFB, NM 87117-5776.

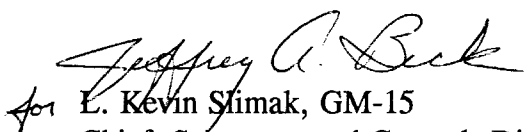
Do not return copies of this report unless contractual obligations or notice on a specific document requires its return.

This report has been approved for publication.



JONATHAN BISHOP, 2Lt
Project Manager

FOR THE COMMANDER



for L. Kevin Slimak, GM-15
Chief, Structures and Controls Division



HENRY L. PUGH, JR., Col, USAF
Director, Space and Missiles Technology
Directorate

The following notice applies to any unclassified (including originally classified and now declassified) technical reports released to "qualified U.S. contractors" under the provisions of DoD Directive 5230.25, Withholding of Unclassified Technical Data From Public Disclosure.

NOTICE TO ACCOMPANY THE DISSEMINATION OF EXPORT-CONTROLLED TECHNICAL DATA

1. Export of information contained herein, which includes, in some circumstances, release to foreign nationals within the United States, without first obtaining approval or license from the Department of State for items controlled by the International Traffic in Arms Regulations (ITAR), or the Department of Commerce for items controlled by the Export Administration Regulations (EAR), may constitute a violation of law.
2. Under 22 U.S.C. 2778 the penalty for unlawful export of items or information controlled under the ITAR is up to two years imprisonment, or a fine of \$100,000, or both. Under 50 U.S.C., Appendix 2410, the penalty for unlawful export of items or information controlled under the EAR is a fine of up to \$1,000,000, or five times the value of the exports, whichever is greater; or for an individual, imprisonment of up to 10 years, or a fine of up to \$250,000, or both.
3. In accordance with your certification that establishes you as a "qualified U.S. Contractor", unauthorized dissemination of this information is prohibited and may result in disqualification as a qualified U.S. contractor, and may be considered in determining your eligibility for future contracts with the Department of Defense.
4. The U.S. Government assumes no liability for direct patent infringement, or contributory patent infringement or misuse of technical data.
5. The U.S. Government does not warrant the adequacy, accuracy, currency, or completeness of the technical data.
6. The U.S. Government assumes no liability for loss, damage, or injury resulting from manufacture or use for any purpose of any product, article, system, or material involving reliance upon any or all technical data furnished in response to the request for technical data.
7. If the technical data furnished by the Government will be used for commercial manufacturing or other profit potential, a license for such use may be necessary. Any payments made in support of the request for data do not include or involve any license rights.
8. A copy of this notice shall be provided with any partial or complete reproduction of these data that are provided to qualified U.S. contractors.

D E S T R U C T I O N N O T I C E

For classified documents, follow the procedures in DoD 5200.22-M, Industrial Security Manual, Section II-19 or DoD 5200.1-R, Information Security Program Regulation, Chapter IX. For unclassified, limited documents, destroy by any method that will prevent disclosure of contents or reconstruction of the document.

DRAFT SF 298

1. Report Date (dd-mm-yy) May 1996		2. Report Type Final		3. Dates covered (from... to) 4/95 to 05/96	
4. Title & subtitle High Performance Ir-Re Composite			5a. Contract or Grant # F29601-95-C-0137		
			5b. Program Element # 62601F		
6. Author(s) Dr Shanjin He			5c. Project # 1602		
			5d. Task # CO		
			5e. Work Unit # EV		
7. Performing Organization Name & Address Ceramic Composites Incorporated 1110 Benfield Blvd, Suites Q-R Millersville, MD 21108				8. Performing Organization Report #	
9. Sponsoring/Monitoring Agency Name & Address Phillips Laboratory 3550 Aberdeen Ave SE Kirtland AFB, NM 87117-5776				10. Monitor Acronym	
				11. Monitor Report # PL-TR-96-1067	
12. Distribution/Availability Statement Distribution authorized to DoD components only; Proprietary Information: May 1996. Other requests for this document shall be referred to AFMC/STI.					
13. Supplementary Notes					
14. Abstract A novel low temperature chemical vapor deposition (CVD) process has been developed for the co-deposition of Ir and Re. The co-deposit was dense and consisted of both Re and Ir with crystallites ranging from 30 Å and 1000 Å in size. A reactive vapor phase was formed between 205 °C and 220 °C, and deposition was carried out onto quartz, graphite and rhenium substrates at between 410 °C and 425 °C. Changes to the processing parameters resulted in an increase in the deposition rate up to 0.8 mil/hour. Various Ir:Re ratios were investigated and compositions between 90%Ir-10%Re and 95%Ir-5%Re were identified as showing the best oxidation resistance at 2000 °C. Application of a 90%Ir-10%Re coating was carried out onto the inside surface of a rhenium matrix, carbon fiber reinforced 25lbf thruster. Densification of the thruster took 51 hours in total and resulted in a composite with 33.9% open porosity. This low temperature CVD technique is generic in its approach and can be applied to deposit a wide range of nano-crystalline metal coatings.					
15. Subject Terms Chemical Vapor Deposition, Vapor					
Security Classification of			19. Limitation of Abstract Limited	20. # of Pages 34	21. Responsible Person (Name and Telephone #) Lt. Bishop (505) 846-9332
16. Report unclassified	17. Abstract unclassified	18. This Page unclassified			

Table of Contents

Table of Contents	iii
List of Figures.....	iv
1. Executive Summary	1
2. Introduction.....	2
2.1 Background	2
2.1.1 Dispersed Phase Composites.....	2
2.1.2 Current Satellite Thrusters	3
2.1.3 Original Iridium-Rhenium Developments.....	5
2.1.4 Advanced Oxidation Resistant Iridium Based Coatings.....	7
3. Project Objectives.....	7
4. Experimental Work Performed.....	7
4.1 Initial Deposition Efforts	7
4.2 Development of Novel Deposition Technique	8
4.3 Codeposition of Ir/Re Oxidation Samples.....	10
4.4 Oxidation Tests	11
4.4.1 Acetylene Torch Tests.....	11
4.5 Characterization of Samples.....	11
4.5.1 X-ray Diffraction Analysis of Codeposited Samples	12
5. Results	12
5.1 Electron Microscopy of Selected Coatings	12
5.2 X-ray Diffraction Analysis of Ir/Re Codeposits	15
5.3 Analysis of the Coatings Following Oxidation	18
5.4 X-ray Diffraction Analysis of Oxidized Samples.....	18
5.5 Fabrication of Fiber Reinforced Ir/Re Thruster.....	21
6. Technical Feasibility.....	23
7. Conclusions and Recommendations.....	24

List of Figures

Figure 1.....	4
Melting Points of Refractory Thruster Candidate Materials to Theoretical Flame temperatures of Various Fuel/Oxidant Combinations	
Figure 2.....	4
Generic Schematic of a Rocket Thruster Highlighting the Major Sections	
Figure 3.....	6
Ir-Re Phase Diagram	
Figure 4.....	6
Changes in Oxidation Rates of Refractory Metals in Relation to Temperature	
Figure 5.....	10
Schematic of the Low-Temperature Deposition System for Iridium Alloy	
Figure 6.....	11
Schematic diagram of oxidation test rig	
Figure 7.....	12
Electron micrograph of Ir/Re co-deposits at (a) atmospheric and (b) 620 torr pressure, illustrating the difference in surface morphology between the two deposits.	
Figure 8.....	13
Energy dispersive spectrum obtained from STEM for the Ir/Re co-deposits at (a) atmospheric and (b) 620 torr pressure, illustrating a difference in the Ir/Re ratios.	
Figure 9.....	14
Electron micrograph of Ir/Re codeposits at (a) atmospheric and (b) 620 torr pressure, illustrating the difference in crystallite size and morphology between the two deposits.	
Figure 10.....	15
Electron transmission diffraction patterns of Ir/Re co-deposits at (a) atmospheric and (b) 620 torr pressure. This clearly illustrates the significant crystallization in the deposit, deposited at a lower pressure.	
Figure 11.....	16
X-ray diffraction pattern for the 95% Ir / 5% Re composition on a rhenium coated substrate.	
Figure 12.....	17
X-ray diffraction pattern for the 90% Ir / 10% Re composition on an uncoated graphite substrate.	

Figure 13.....	18
Photograph of the oxidized samples.	
Figure 14.....	19
X-ray diffraction pattern for the 95% Ir / 5% Re composition on a rhenium coated substrate after oxidation testing.	
Figure 15.....	20
X-ray diffraction pattern for the 90% Ir / 10% Re composition on an uncoated graphite substrate after oxidation testing.	
Figure 16.....	21
Section of NASA 25lbf thruster.	
Figure 17.....	22
Schematic of the rhenium deposition system.	
Figures 18 and 19.....	23
Photographs of the 25lbf thruster produced, showing the carbon braided mandrel before and after coating with Re and Ir/Re composition.	

1. Executive Summary

Iridium coated Re thrusters have historically been developed to improve the life cycle and efficiency of spacecraft propulsion systems by improving oxidation resistance and significantly reducing, and hopefully eliminating, the need for cooling during operation with high energy, bipropellant fuels. The lifetime of present Re thrusters, which are coated with an Ir layer which acts as a barrier against oxidation of the Re, is limited by diffusion of Re into the hot Ir surface. Diffusion takes place along the oriented grain boundaries of the large Ir grains, and once the concentration of Re exceeds 20%, rapid oxidation and structural failure takes place.

The objective of this Phase I proposal was to establish the optimum composition for a co-deposition of microcrystalline Ir and Re, which has improved oxidation resistance and which could be applied to a carbon fiber preform to reduce the overall thruster weight and the total material costs (which are significant for Re and Ir).

This Phase I research resulted in a technical breakthrough. A novel low temperature process was developed which co-deposits dense films of both Re and Ir with a crystallite size between 30 Å and 1000 Å. Various Ir:Re ratios were investigated and compositions between 90%Ir-10%Re and 95%Ir-5%Re were identified as showing the best oxidation resistance at 2000 °C. Changes to the processing parameters resulted in a deposition rate of 0.8 mil/hour. A 25 lbf thruster has been fabricated from carbon fibers infiltrated with Re and coated with a co-deposit of 90%Ir-10%Re on the inner surface. This thruster will be sectioned to reveal the microstructure and depth of penetration of the Ir-Re codeposit.

The result of improved oxidation resistance may be several years of additional usable satellite life. With typical satellite fabrication and launch costs exceeding \$250M, an additional 2 years of service life could be worth \$20-40M.

The application of this coating to carbon fiber preforms considerably reduces the amount of metal required to fabricate the thrusters resulting in lower fabrication costs and a 30% reduction in the weight. The unique capability to deposit oxidation resistant Ir-Re codepositions at low temperatures offers great flexibility for a wide spectrum of aerospace applications. These include protective coatings for C/C composites, monolithic rhenium structures or coatings, or as a refractory infiltrant matrix for long-life fiber reinforced composites. Moreover, the codeposition approach could be extended to a wide range of unique refractory, oxidation resistant compounds, such as Ir-Al and Ir-La, which could provide significant future rocket and turbine engine propulsion systems.

2. Introduction

The service life of current technology metal thrusters can be measured in tens of hours of operation. Refractory metal or ceramic matrix thrusters have the potential of hundreds of hours of service life with the possibility of service life in the thousand hour range. Extended service life becomes important to such long life systems as low earth space platforms which will have 20 or 30 year usable lifetimes or longer. A potentially attractive space station propulsion approach involves shipping water to the platform from earth and electrolyzing the water into hydrogen and oxygen in orbit using solar photovoltaic power and feeding the orbital stabilization thrusters gaseous hydrogen and oxygen propellants. A 2000 hour life thruster would be desirable so that new thrusters do not have to be shipped periodically to the station. Since water electrolytically produces stoichiometric combustion propellants, thrusters that are capable of operating at near 2750 °C service conditions are needed to maximize the achievable specific impulse.

One of the near term major applications in the commercial sector are propulsion system thrusters for communication satellites. Present niobium (columbium) thrusters operate with typical fuel/oxidizer ratios that are well below stoichiometry to keep the silicide-coated thruster walls below a 1400 °C surface temperature. The use of near stoichiometric combustion conditions would improve thruster efficiency and extend the station-keeping lifetime of commercial satellites by several years. Two years of additional service life could be worth \$20-40M, given the typical satellite fabrication and launch costs which can exceed \$250M.

Iridium coated Re thrusters have historically been developed to improve the life cycle and efficiency of spacecraft propulsion systems, by increasing the operational temperature, oxidation resistance and significantly reducing, and hopefully eliminating the need for cooling during operation with high energy, bipropellant fuels. The lifetime of present Ir coated Re thrusters is limited by diffusion of Re into the hot Ir surface. Diffusion takes place along the oriented grain boundaries of the large Ir grains, and once the concentration of Re exceeds 20% at the inner surface of the combustion chamber, rapid oxidation takes place. The fabrication of a stable micro-crystalline co-deposit of Ir and Re would improve the oxidation resistance by inhibiting the diffusion of Re along Ir grain boundaries.

2.1 Background

2.1.1 Dispersed Phase Composites

The use of composites is frequently preferred over single phase materials due to the ability to vary and control the material properties.¹ Several reasons exist for the current interest in composites. For ceramics, the major thrust is to reduce brittleness, i.e., increase the fracture toughness thereby making these materials suitable for engineering applications where their exceptional high temperature properties and oxidation resistance can be utilized. Extensive progress has been made in improving mechanical properties of particulate, whisker, and fiber reinforced ceramics prepared by chemical vapor deposition (CVD). Other techniques - powder blending and subsequent sintering, or hot pressing of composite materials - have also been successful, but typically their toughness is not as high as that obtained via CVD of continuous fiber preforms. Continuous fiber reinforced ceramic matrix composites offer exceptional resistance to thermal shock, but at high temperatures

¹W. J. Lackey, A. W. Smith, D. M. Dillard, D. J. Twait, "Codeposition of Dispersed Phase Ceramic Composites," Proceedings of the American Ceramic Society, Cocoa Beach, 1987, p. 1008.

suffer from severe oxidation of the reinforcing fibers, which results in a loss of strength. At 2200 °C graphite has the highest strength of all materials, but if it is to be used in oxidizing conditions at these temperatures the individual fibers must be protected from oxidation.

Iridium-rhenium coatings offer enhanced oxidation resistance which will allow the potential of these high temperature fiber reinforced materials to be realized. Deposition of the composite coatings is also of interest due to the possibility of tailoring the coefficient of thermal expansion of the coating. Increased coating toughness and strength, and control of the thermal expansion mismatch between the substrate and coating should result in superior coating adherence. Chemical vapor deposition is a very versatile process which is applicable to a large number of matrix-dispersed chemical combinations. At present the growth of most coatings via CVD typically promotes the growth of large columnar grains perpendicular to the substrate. Porosity, gases and other imperfections to crystal growth will accumulate at these grain boundaries and severely degrade the properties and performance of the resulting coating. In thin coatings, typically less than 1000Å, where columnar growth has not yet become established, measured coating properties² have been significantly improved. Ideally, the CVD process should provide uniformly dispersed small crystallites in order to improve the coating properties and attain high strength.

CVD codeposited film morphology is influenced by several factors. The major processing parameters which influence the morphology are the supersaturation of the reacting gaseous species and substrate temperature. Large degrees of supersaturation favor deposits consisting of randomly oriented, small grains. Low degrees of supersaturation hinder nucleation and favor growth of particular crystallographic orientations. This condition is representative of elongated grains and whisker growth. Simultaneous nucleation on the substrate surface of two distinct materials, as expected in the case of Re and Ir codeposits, results in a bimodal microstructure. This is due to a competition between the two phases for available surface sites for subsequent nucleation and growth. This behavior has been seen in codeposited systems including C + SiC and AlN + BN. The bimodal behavior can be altered by changing processing conditions to enhance or reduce the relative amount or structure of each phase. For the Ir/Re thruster, small particles of Re will suppress the typical columnar growth of the Ir phase, leading to improved fracture and erosion resistance.

2.1.2 Current Satellite Thrusters

Almost all liquid rocket thrust chambers in service are currently fabricated using niobium with a metal silicide coating for oxidation protection. This thruster is drastically limited by its low maximum operating temperature (1125-1625 °C), which is a result of the volatilization of SiO from the silicide coating and is exacerbated by cracking and spalling of the coating due to thermal cycling from room to elevated temperatures. Because of the low operating temperature, a significant amount of the liquid propellant must be injected into the combustion chamber for wall cooling. This process, called fuel film cooling, greatly reduces the amount of fuel that burns to completion, resulting in an inefficient and costly operation. Loss of the protective SiO₂ film on the NbSi₂ surface and degradation of the coating due to thermal cycling increases the likelihood of further oxidation of the niobium underlayer. The theoretical flame temperature of various oxidant-fuel combinations that NASA and the military services are experimenting with are shown in Figure 1. The lifetime of typical niobium coated thrusters must be improved for aerospace and military applications. Since very small increases in temperature result in a dramatic decrease in lifetime, present efforts to produce high temperature, oxidation resistant niobium thrusters have focused on improving coating performance and fuel cooling.

²R.W. Siegal and G.E. Fougere, Mater. Res. Soc. Symp. Proc. Vol 362, 1995. pp. 219.

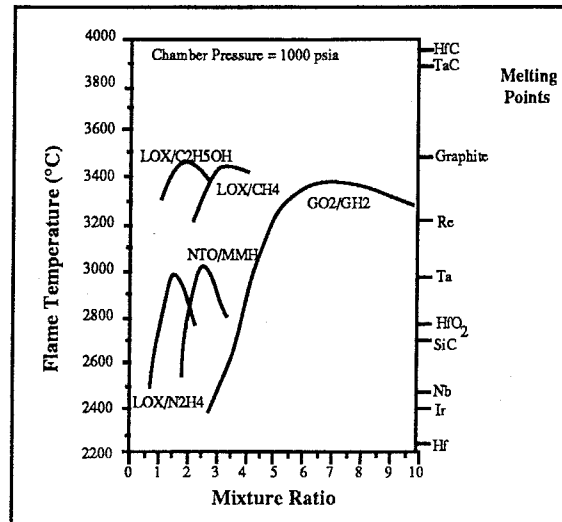


Figure 1. Melting points of refractory thruster candidate materials to theoretical flame temperatures of various fuel/oxidant combinations.

Thrusters fabricated from composites are attractive materials since they offer a potential reduction in weight and for certain material systems offer the potential for radiation cooling, even near stoichiometric combustion fuel mixtures. Optimization of these materials systems could provide a universal approach to uncooled thrusters capable of maximum efficiency. The forward convergent section of the thruster is the combustion chamber where the fuels are introduced and combusted. This section is placed under a combination of hoop tension, compression, and shear stresses. As the hot combustor gases pass through the throat and into the exit cone, the gases cool rapidly due to adiabatic expansion. The combustion chamber, throat, and exit cone of a NASA Lewis 25 lbf liquid rocket thruster is shown in the schematic of Figure 2.

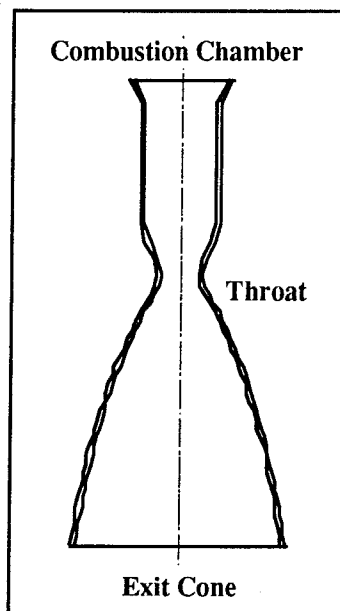


Figure 2. Generic schematic of a rocket thruster highlighting the major sections.

A fiber reinforced ceramic matrix composite should provide additional strength and chamber pressurization capabilities. Two dimensional triaxial braided fiber architectures have demonstrated the best combination of hoop, axial and radial tensile, and shear strength properties for rocket thrusters. In the past, ceramic composites tested for thruster applications have not been capable of holding a chamber pressure above approximately 30 psi. Recent results however, using a novel sandwich constitution³ have demonstrated a chamber pressure of 75 psi during testing even though the CMC density was less than 60%. This thruster consisted of dense carbide layers on the surface and near-surface regions and a porous carbide structure on the interior of the carbon fiber preform. The use of an engineered coating system which permits higher temperature operation with minimal cracking is expected to improve the high temperature cyclic fatigue (crack propagation resistance) and long term oxidation stability of fiber reinforced composite thrusters.

2.1.3 Original Iridium-Rhenium Developments

Extensive thruster development and testing of Ir coated Re monolithic thrusters has been performed by Aerojet Propulsion Division as part of a NASA funded effort.⁴ A system composed of an iridium coating over a rhenium liner was the focus of development efforts for several reasons. First, Re and Ir both have high melting points of 3186 °C and 2447 °C, respectively. Second, the thermal expansion coefficient of each metal is similar. A final key advantage is the exceptional oxidation resistance of iridium. A summary table of the physical properties of iridium and rhenium is presented in Table I. The Ir-Re phase diagram, shown in Figure 3, indicates the solid solubility of the two materials at rhenium percentages below 30 wt %.

Table I. Physical properties of Iridium and Rhenium.

	(T Melt °C)	Linear Thermal Exp. 10^6 K^{-1}	Heat Capacity g/cm K	Thermal Conductivity w/cm•k
Ir	2447	6.4	0.131	1.47
Re	3186	6.2	0.137	0.479

The oxidation rate of several refractory metals is shown in Figure 4. This plot highlights the excellent oxidation resistance of iridium, and the relatively poor oxidation resistance of rhenium. A series of Ir-Re billets of different compositions fabricated by hot pressing at Aerojet were oxidized and showed that with Re compositions greater than 20 wt. %, catastrophic oxidation occurred as the temperature was raised above 1500 °C in air. **This behavior was attributed to the large grains of iridium within the structure providing a diffusion pathway for Re and oxygen mobility.**

³M. Patterson, S. He, L. Fehrenbacher, B. Reed and J. Hanigofsky, "Advanced HfC-TaC Oxidation Resistant Composite Rocket Thruster" Conf. Proc. ASM Materials Week, Cleveland, OH. 30th Oct - 2 Nov.

⁴J.R. Wooten and P.T. Lansaw, "High Temperature Oxidation-Resistant Thruster Research," NASA, #185233, February 1990.

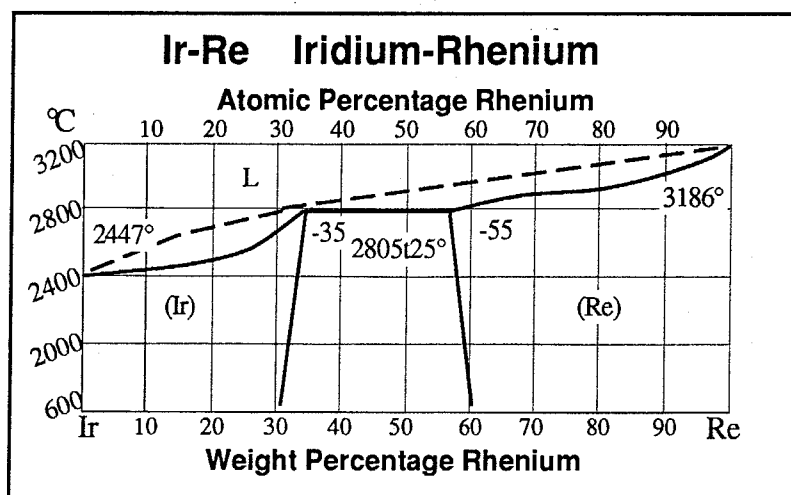


Figure 3. Ir-Re Phase Diagram.

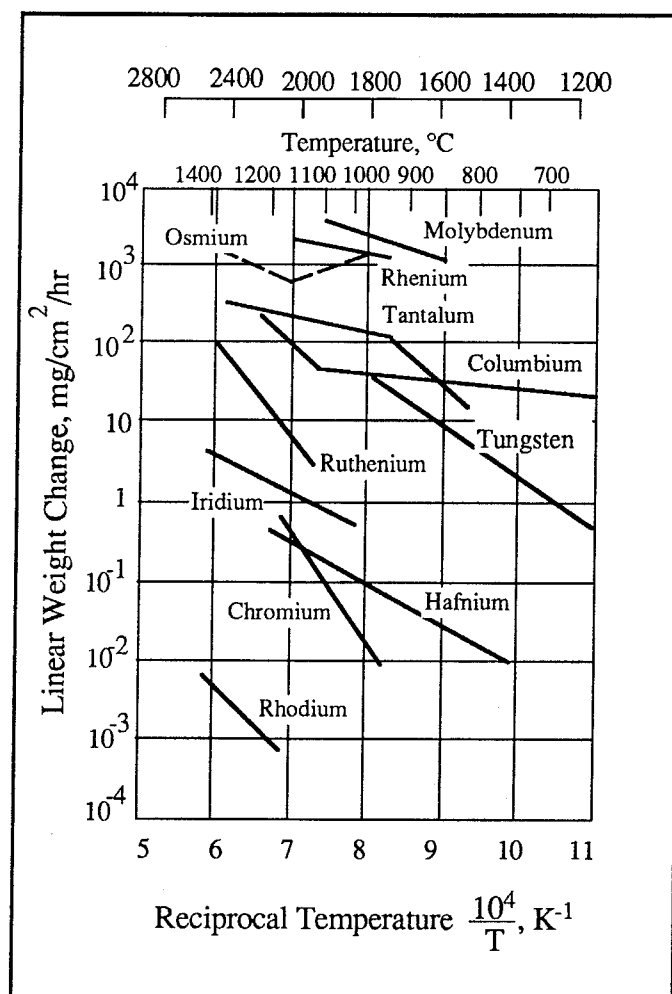


Figure 4. Changes in oxidation rate of refractory metals in relation to temperature.

2.1.4 Advanced Oxidation Resistant Iridium Based Coatings

Another attempt to improve the lifetime of iridium coated rhenium thrusters was based on sol coated oxide monolithic layers by Ultramet⁵. The refractory oxides hafnia and zirconia with different coating thicknesses were deposited onto the iridium. The testing and evaluation of these oxide-coated Ir-Re thrusters has been carried out by Brian Reed of NASA Lewis⁶. The thick-walled coatings did provide a temperature drop across the oxide layer, but macro cracking and spalling occurred in thick-walled coatings and burn-throughs in the throat region were common even with the more tenacious of these oxide coatings. More recently⁷, the thin coatings have been shown to be tenacious and have provided significant protection against oxidation of the Ir/Re substrate.

3. Project Objectives

The main technical objective of the Phase I effort involved process development for a series of Ir-Re codeposited compositions (20 wt.% Re and less), to demonstrate that their oxidation resistance was equivalent to or better than pure Ir. Specific technical goals included:

- Establish the oxidation resistance and microstructural relationships between several CVD codeposits of Ir-Re
- Fabrication of a 25 lbf carbon fiber reinforced rocket thruster using the codeposited stoichiometry with the best oxidation protection performance.

4. Experimental Work Performed

4.1 Initial Deposition Efforts

The major obstacle to producing iridium films through chemical vapor means has been the difficulty of forming iridium compounds with a stable vapor phase. Our initial attempts at deposition of iridium and rhenium were based on the in situ chlorination of the metals. Most metals can be deposited by direct chlorination with gaseous Cl_2 at temperatures between 500 °C and 1100 °C. The chloride vapors are subsequently reduced with H_2 at a higher temperature to deposit the metals. Considerable effort was directed towards the codeposition of iridium and rhenium by this method. It was found that this process does not and can not work with iridium because the vapor pressure of IrCl_3 is too low at temperatures between the formation temperature (500 °C) and the decomposition temperature (760 °C), to produce an appreciable quantity of vapor phase. The Phase I research was originally based on this method of deposition, but after the failure of the initial high temperature codeposition attempts, an alternative deposition method was sought.

A thorough investigation of the literature concerning the chemical vapor deposition of iridium from various organic and inorganic precursors revealed several techniques.

⁵Q. Jang, R.H. Tuffias, R.La Ferla, and N.M. Ghoniem, "Design, Analysis, and Fabrication of Oxide-Coated Iridium/Rhenium Combustion Chambers," Proc. JANNAF Propulsion Meeting, Monterey, CA. 15-19 Nov 1993.

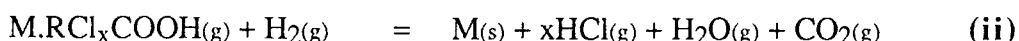
⁶B. D.Reed, "Testing and Evaluation of Oxide-Coated Iridium/Rhenium Chambers," Proc. JANNAF Propulsion Meeting, Monterey, CA. 15-19 Nov 1993.

⁷B.D. Reed, Private Communication. 1996.

Several sources involved the use of metallorganic precursors⁵ such as iridium acetylacetonate. Others focused on the deposition of iridium using cyclooctadiene iridium cyclopentadiene, cyclooctadiene iridium acetylacetonate and iridium fluoride⁸. Production of iridium metal from its fluoride is an analogous process to the production from the chloride. While this process produces iridium films, the hydrogen fluoride produced as a by-product of the depositing reaction was found to attack the graphite substrates resulting in pitted, poor quality, deposits. Deposition using cyclopentadienyliridium cyclopentadiene produces good quality films. The starting materials are expensive and their availability is limited. This process also yields very low deposition rates and for these reasons these processes was determined not to be economically feasible.

4.2 Development of Novel Deposition Technique

The process which finally resulted in suitable iridium and Ir-Re codeposited films is based on the vaporization of IrCl_3 and other metal chlorides, through the in situ formation of metallic carbonyl hydroxychloride vapor species⁹. The development of this codeposition process, which resulted from an intensive experimental phase I effort, has widespread potential for the codeposition of refractory metals with unique properties. This process has been found to produce uniform and homogeneous deposits. The deposition rates are reasonable and the raw materials are relatively reasonably priced. The volatile species are formed by the reaction of a volatile hydroxyl containing ligand and carbon monoxide with the iridium chloride in a quasi-fluidized bed reactor. The actual specific species have not been well characterized, but it is a two stage reaction, in which a volatile phase containing the "metals" for codeposition is formed, followed by the reduction of this volatile phase and the codeposition of the metallic phases. The two separate stages of the reaction are as follows:



The hydroxyl phase can range in composition from water to larger molecular mass alcohols, and the deposition rate of the codeposit seems very sensitive to the vapor pressure of this particular phase. In the Phase I research, an alcohol with a high vapor pressure (either ethanol or propanol) was used and the rate was controlled by the use of an inert carrier gas (Ar), which was bubbled through the liquid alcohol.

This procedure requires a balance between reactor geometry and gas flow rates to provide a quasi-fluid state in the chloride powder bed and adequate residence time of the organo-ligand species. Hydrogen is used in the reduction of the volatile vapor phase. The maximum temperatures achieved in the reactor are below 450 °C. Control of the flow of the various gas phase components has been found to be a critical parameter to successfully deposit codeposited metallic films by this method.

Several process variables were investigated in order to maximize the deposition rate and compositions. The experimental design matrix shown in Table II reveals the broad range of process parameters investigated.

⁸B.A. Macklin and P.A. LaMar, "Development of Improved Methods of Depositing Iridium Coatings on Graphite," AFML Tech. Rep.# AFML-TR-67-195, part II, Wright Patterson AFB OH, Oct 1968.

Table II Process variables for optimization of codeposited Ir/Re coatings.

	Reactor Temperature (°C)	Substrate Temperature (°C)	Gas Composition and Flow Rate (sccm)	Pressure (torr)	Deposition Time (hour)
Upper Limit	220	425	[R-OH] 3 [CO] 100 [H ₂] 400 [Ar] 30	760	16.0
Lower Limit	205	410	[R-OH] 3 [CO] 100 [H ₂] 100 [Ar] 30	100	1.0

The special low-temperature deposition system which was developed during the Phase I effort at CCI is illustrated in Figure 5. This is a two stage process in which the temperature of both stages are independently controlled. In this technique, the Ir and Re chloride powders are placed as dispersed solid powders into a graphite holder. The vaporization gases (carbon monoxide and ethyl alcohol) are passed through the chloride powder bed and the volatile organo-ligand species is formed. The alcohol flow rate is determined by the flow rate of an inert gas (Ar) and the vapor pressure of the alcohol. The generation of the volatile vapor phase corresponding to equation (i), takes place typically between 205° and 220° C. The sample holder and tube wall are heated by external resistance heating in order to avoid condensation of the vapor phase. The organo-ligand vapor is injected into the deposition zone through a small quartz tube. For codeposition of the refractory metals corresponding to equation (ii), on a flat substrate, the substrate is placed on the surface of a graphite sample holder which is heated by a cartridge type resistance heater. The deposition temperature is measured by a thermocouple imbedded in the holder. Hydrogen gas, which is introduced separately, reacts with the volatile species at the surface of the substrate and the metals are deposited on the substrate. The waste gases (H₂O, HCl, and CO₂) are exhausted to the scrubber system, where they are neutralized and disposed of.

Ethyl alcohol gas is produced with a standard liquid vaporizer. A metered flow of argon is bubbled through the liquid ethyl alcohol. The mixture of Ar and alcohol gases are mixed with carbon monoxide. The mixed gases are fed into the sample powder holder. The desired flow rate of the alcohol is controlled by adjusting the argon flow rate in proportion to the vapor pressure of the alcohol at ambient temperature.

The iridium carbonyl hydroxychloride vapor phase reacts with hydrogen gas at elevated temperature in the deposition zone to produce iridium coatings. The temperature in the substrate deposition zone, while higher than that in the volatilization zone, is low. The deposition zone temperature was varied between 410 ° and 425 °C which is considerably less than with conventional CVD where the deposition temperature is usually about 1100 °C. Because of the low deposition temperature, the grain size of the co-deposited materials is in the nanoscale range. Thermodynamic studies indicate that this low-temperature CVD technique is a generic CVD method which can be applied to co-deposition of a wide range of alloy systems.

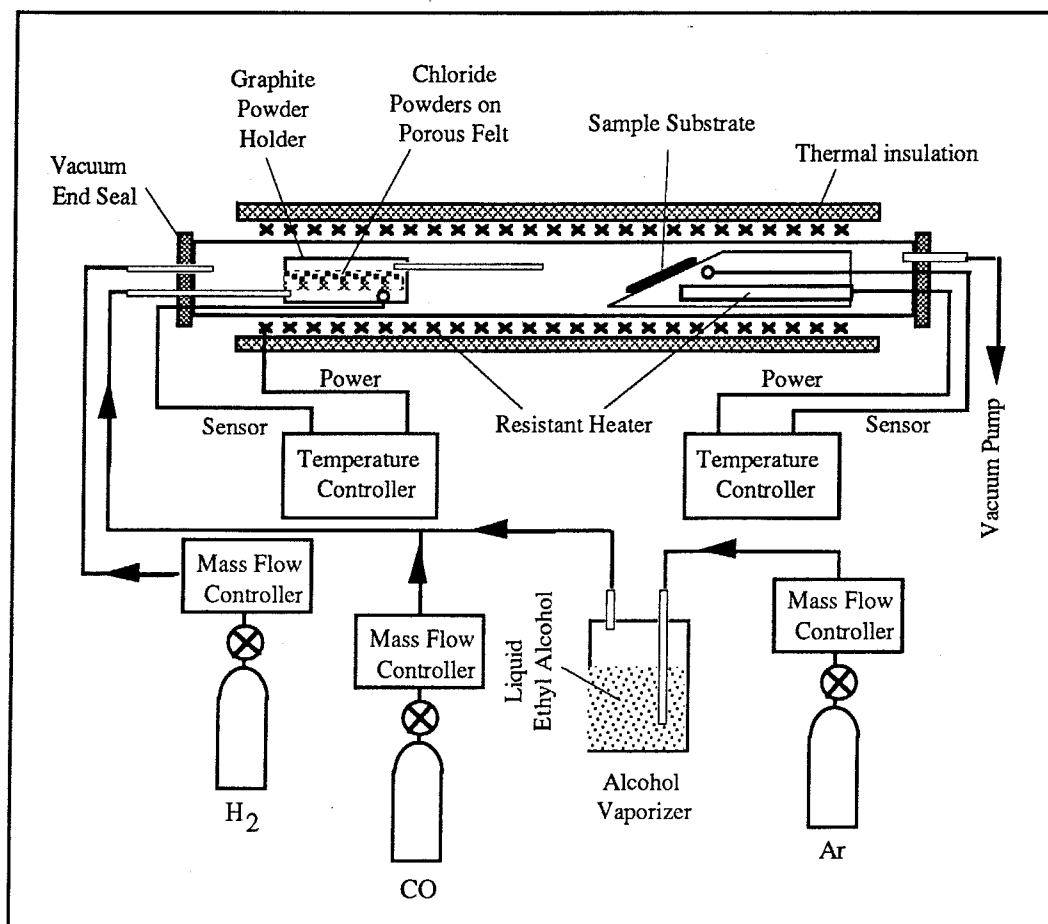


Figure 5 Schematic of the low-temperature deposition system for iridium alloy

The wide range of processing variables which were investigated in this Phase I research enabled optimum conditions for the codeposition of dense Ir/Re coatings to be achieved. Following the original attempts at the direct chlorination of Ir and Re, approximately 40 experiments were performed to identify the important process parameters and enable a dense tenacious codeposition to be achieved. Improved deposition rates were observed with a reaction chamber temperature of 210 °C and substrate temperature of 425 °C. The deposition rate was strongly dependent on the hydrogen flow rate and at a flow rate of 200 sccm, produced the highest codeposition rates. The deposition rate was also seen to increase with increasing pressure up to approximately 630 torr. No further increase was observed at higher pressures.

4.3 Codeposition of Ir/Re Oxidation Samples

Seven samples with different Ir/Re compositions were produced for oxidation testing. The CVD coatings were applied to graphite substrates with dimensions 1" square by 1/8" thick. Three of the samples were coated with 0.05" thick CVD rhenium prior to deposition of the Ir/Re coating. The compositions of the coatings on these three samples were 95% Ir / 5% Re ; 90% Ir / 10% Re ; and 80% Ir / 20% Re, respectively. An additional four samples were deposited on uncoated graphite. The compositions of the coatings on these samples were 100% Ir / 0% Re ; 95% Ir / 5% Re ; 90% Ir / 10% Re ; and 80% Ir / 20% Re respectively.

The coatings for oxidation testing were produced at 630 Torr pressure. The flow rates of the reacting gases H_2 , Ar, CO and C_2H_5OH were 200, 30, 100 and 3 sccm, respectively. Each deposition run was four hours, which resulted in a coating thickness of approximately 0.003 inches.

4.4 Oxidation Tests

4.4.1 Acetylene Torch Tests

Oxidation tests were performed on the seven test samples. An oxygen-acetylene torch was used to bring the surface temperature of the coating to 2000 °C. The samples were mounted on a sample holder, one half of the surface of the samples was protected with a graphite shield. The samples were translated horizontally under already burning flame of the O_2 - C_2H_2 torch as shown in Figure 6. A two-color pyrometer was applied to monitor the surface temperature of the sample. The duration of the exposure to the flame was 30 seconds. The seven samples described above were tested under the same conditions.

After the oxidation test, a close visual and microscopic examination was performed to observe the changes to the surfaces. Post-oxidation x-ray diffraction scans of each sample were also performed.

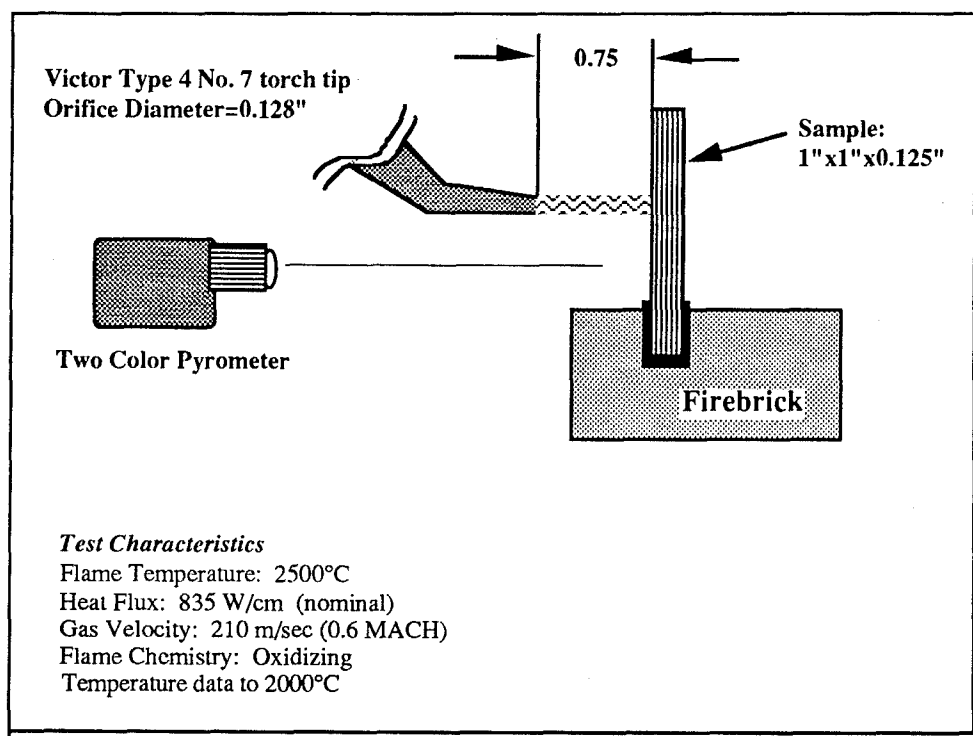


Figure 6. Schematic diagram of oxidation test rig.

4.5 Characterization of Samples

The as-deposited coatings were characterized by x-ray diffraction to establish the degree of crystallinity and the crystalline phases present, and by electron microscopy to see the morphology of the coatings.

4.5.1 X-ray Diffraction Analysis of Codeposited Samples

The deposited samples were characterized by X-ray diffraction using a Philips 1700 series x-ray diffractometer. The parameters used for the diffractometer scans of the samples are tabulated in Table III.

Table III. X-ray diffractometer settings used.

Radiation	Cu $\alpha\alpha$ @ 1.5406 Å
Scan range	10° - 80° 2 θ
Voltage	40 kV
Amperage	25 mA
Beam slit & Receiving slit	1° & 0.1° respectively
Scan speed	2 x 2 θ / min
Time constant	2 sec.
Full scale	200 counts/sec.

5. Results

Selected samples were analyzed by visual inspection, electron microscopy and by X-ray diffraction. The results are summarized in the next section.

5.1 Electron Microscopy of Selected Coatings

Selected samples were analyzed by scanning and transmission electron microscopy (SEM Joel 840, and TEM Philips CM20). Scanning electron microscopy indicated the

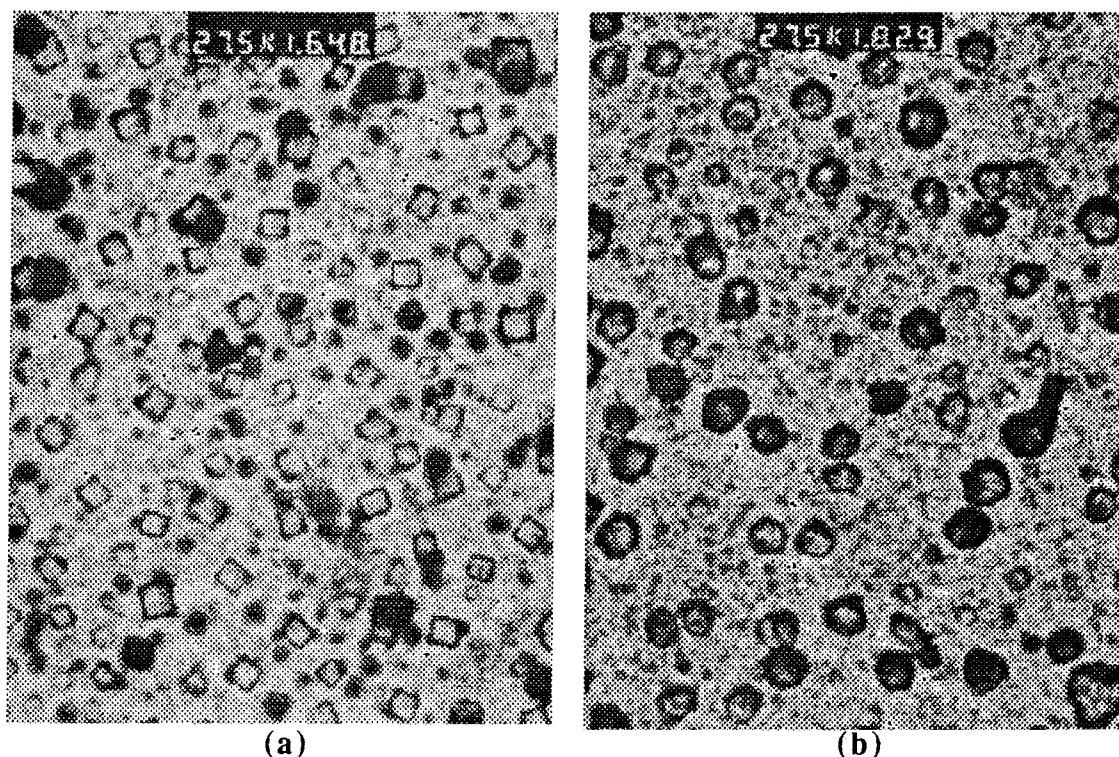


Figure 7. Electron micrograph of Ir/Re co-deposits at (a) atmospheric and (b) 620 torr pressure, illustrating the difference in surface morphology between the two deposits.

coating consisted of a collection of crystals on a dense substrate. At atmospheric pressure these crystals appeared cubic, ranging in size from approximately $0.05\mu\text{m}$ to $0.2\mu\text{m}$ as shown in Figure 7(a). At lower pressures (620 torr), these crystals appeared more rounded in form but still had the same crystallite size distribution as the deposits at higher pressures as shown in Figure 7(b).

Energy dispersive spectrum (EDS obtained from STEM) of the relative Ir and Re concentrations obtained for coatings deposited at atmospheric and 620 torr pressure, indicate a difference in the two compositions. At atmospheric pressure the ratio of Re to Ir is approximately 55:45, as shown in the spectrum in Figure 8(a). This estimate is based on the peak heights and assumes similar outer electron binding energies, which is a reasonable assumption since these elements are very close in atomic number, (75 and 77 respectively). At lower pressures, the Re:Ir ratio changes to approximately 32:68, as shown in Figure 8(b), indicating a considerable increase in the amount of Ir present. The presence of Cu and C is due to the Cu grid onto which the films are deposited and a carbon coating on the grid. It appears as though both coatings are contaminated by a few wt% Fe, which cannot be accounted for at this time.

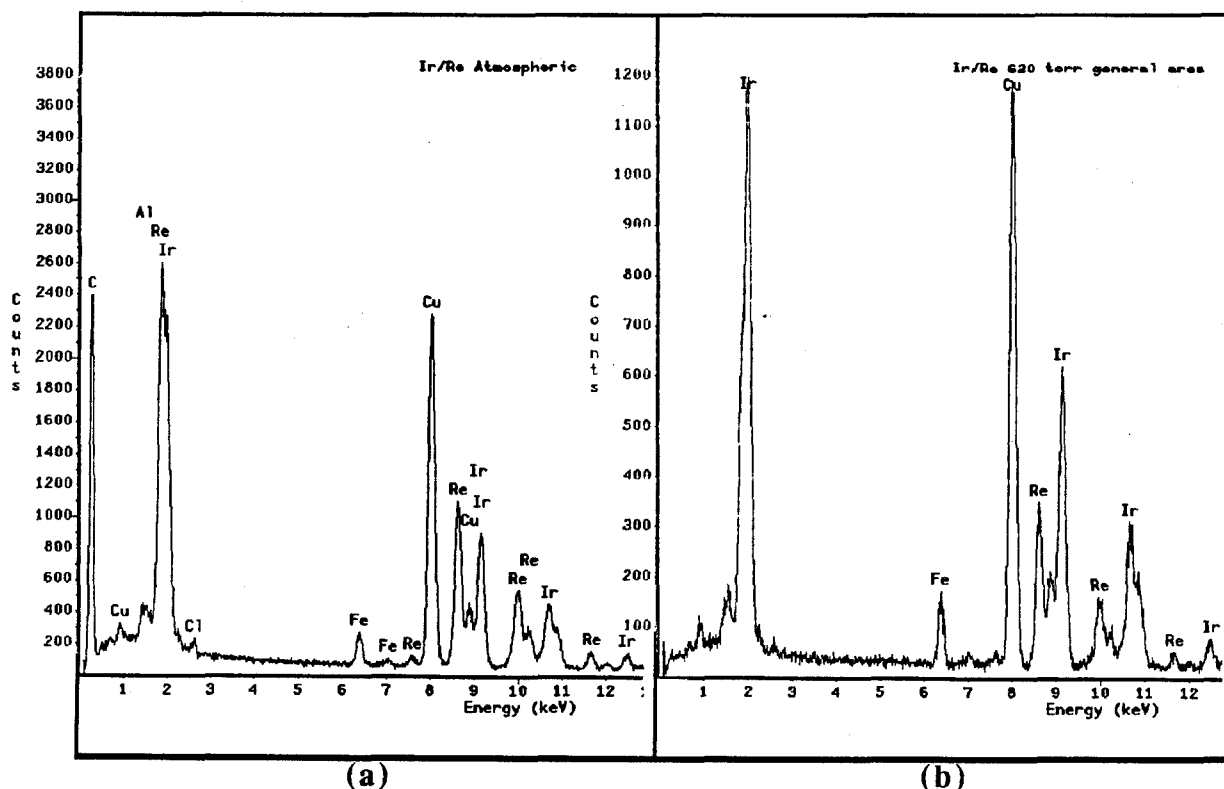


Figure 8. Energy Dispersive Spectrum Obtained from STEM for the Ir/Re co-deposits at (a) atmospheric and (b) 620 torr pressure, illustrating a difference in the Ir/Re Ratios.

Transmission electron microscopy revealed a more accurate microstructural assessment of the films. At atmospheric pressure, the apparently dense substrate can be seen to consist of crystallites ranging in size from approximately 30\AA to 180\AA as shown in Figure 9(a). The larger structures originally observed by SEM appear to be hollow cubic frameworks growing perpendicular to the substrate. It is interesting to note that in these coatings deposited at atmospheric pressure, codeposition occurs preferentially onto the major [100], [010] or [001] lattices of Ir forming the characteristic box type structure. This deposition occurs from a coating that is Re rich. At lower deposition pressures (620 torr),

the crystallite size is larger ranging in size from approximately 40Å to 1000Å, and the larger structure observed by SEM has lost its cubic form and appears more rounded as shown in Figure 9(b). It is probable that this change in the morphology is predominantly due to the competing surface nucleation sites, i.e. the relative concentrations in Ir and Re rather than the small change in pressure between atmospheric and 620 torr.

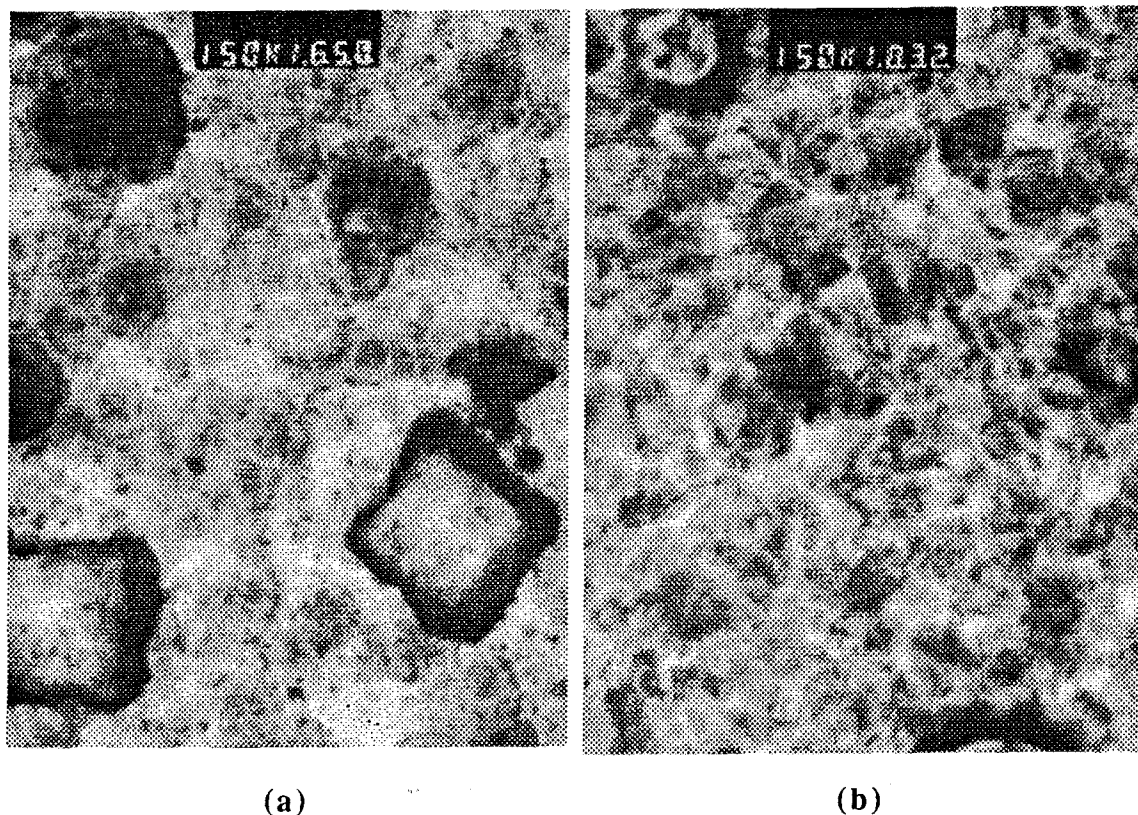


Figure 9. Electron micrograph of Ir/Re co-deposits at (a) atmospheric and (b) 620 torr pressure, illustrating the difference in crystallite size and surface morphology between the two deposits.

Transmission diffraction patterns for these two films deposited at atmospheric and 620 torr are shown in Figure 10 (a) and (b) and reveal the difference in crystallinity. Figure 10(a), deposited at atmospheric pressure, shows an amorphous (nanocrystalline), ring pattern, compared with Figure 10(b) deposited at 620 torr, which shows a ring pattern and individual crystal diffraction spots. At atmospheric pressure the deposit is completely nano-crystalline or amorphous, and the deposit at 620 torr contains a bimodal structure of nano-crystalline or amorphous phases plus a well crystallized phase.

The information collected from these diffraction patterns is not accurate enough to determine lattice spacings for the individual crystallites, but it appears from the pattern of the coating deposited at 620 torr, that all the diffraction rings for both Ir and Re are present, indicating that this is most probably a true codeposit, rather than a solid - solution between Re and Ir.

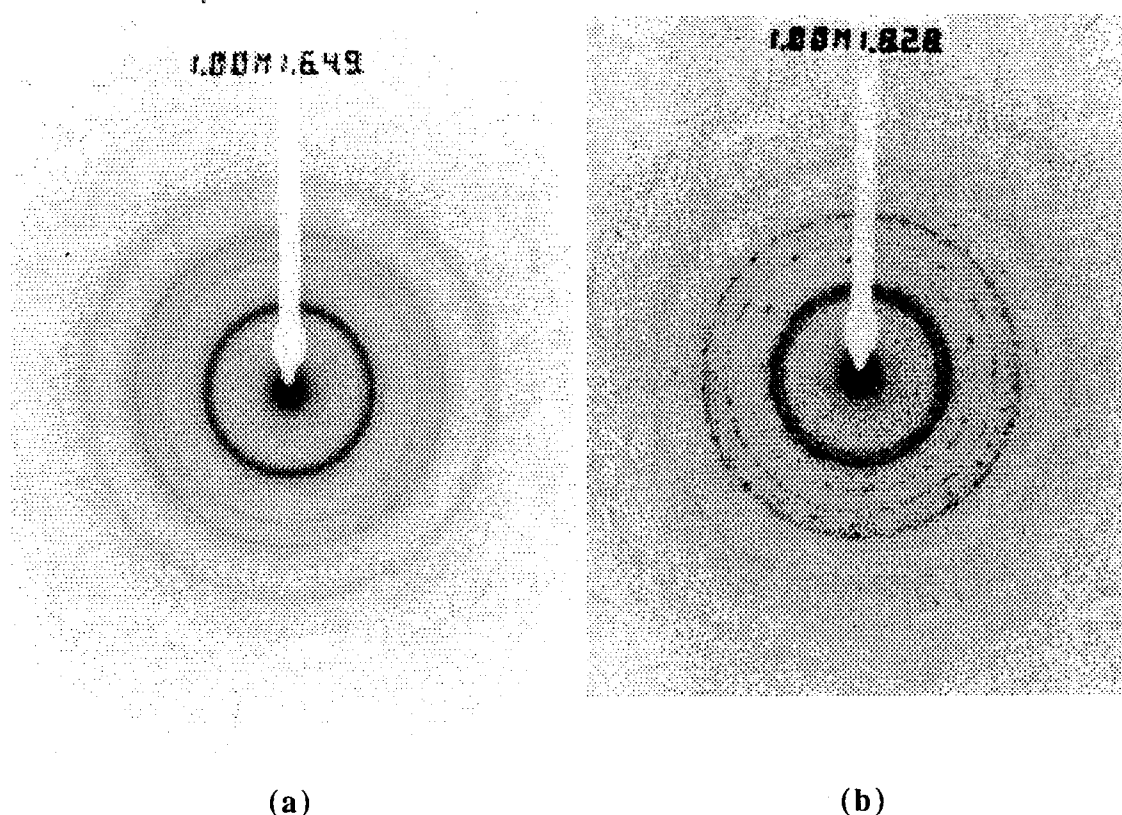


Figure 10. Electron Transmission Diffraction patterns of Ir/Re co-deposits at (a) atmospheric and (b) 620 torr pressure. This clearly illustrates the significant crystallization in the deposit deposited at a lower pressure.

Analysis of the individual crystals was not possible in the present study, but the presence of separate diffraction rings for both Re and Ir tends to indicate that the metals are deposited stoichiometrically rather than forming a solid-solution.

5.2 X-ray diffraction analysis of Ir/Re co-deposits

The x-ray diffraction pattern for the sample with 95% Ir / 5% Re composition on rhenium coated substrate is shown in Figure 11. The small broad peaks at $47.3^\circ 2\theta$ and $69.0^\circ 2\theta$ are from iridium [200] and [220] reflections respectively. The remainder of the peaks are from the rhenium substrate. The major iridium peak at $40.6^\circ 2\theta$ [111] is obscured by the rhenium [002] reflection at $40.5^\circ 2\theta$. The peaks of the codeposited material are broadened and diminished in height due to the small crystallite size.

The x-ray diffraction pattern for the sample with 90% Ir / 10% Re composition on an uncoated graphite substrate is shown in Figure 12. The distinct broad peaks at $47.3^\circ 2\theta$ and $69.0^\circ 2\theta$ are from the iridium [200] and [220] reflections respectively. The only indication of rhenium is at $42.9^\circ 2\theta$, which corresponds to the major rhenium [101] reflection. The remainder of the peaks are from the graphite substrate. Again the peaks of the codeposited material are broadened and diminished in height due to the small crystallite size.

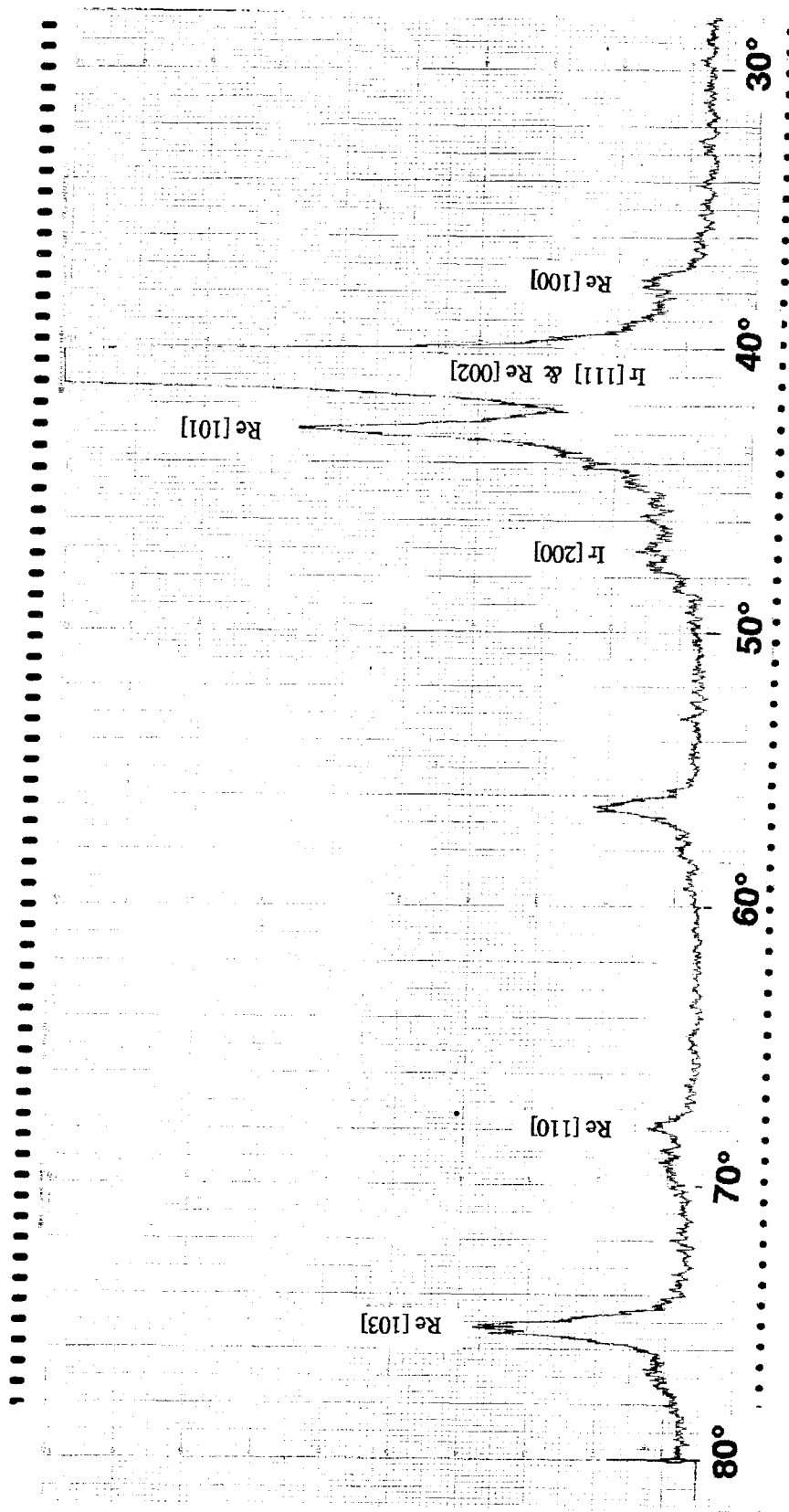


Figure 11

X-ray diffraction pattern for the 95% Ir / 5% Re composition on rhenium coated substrate.

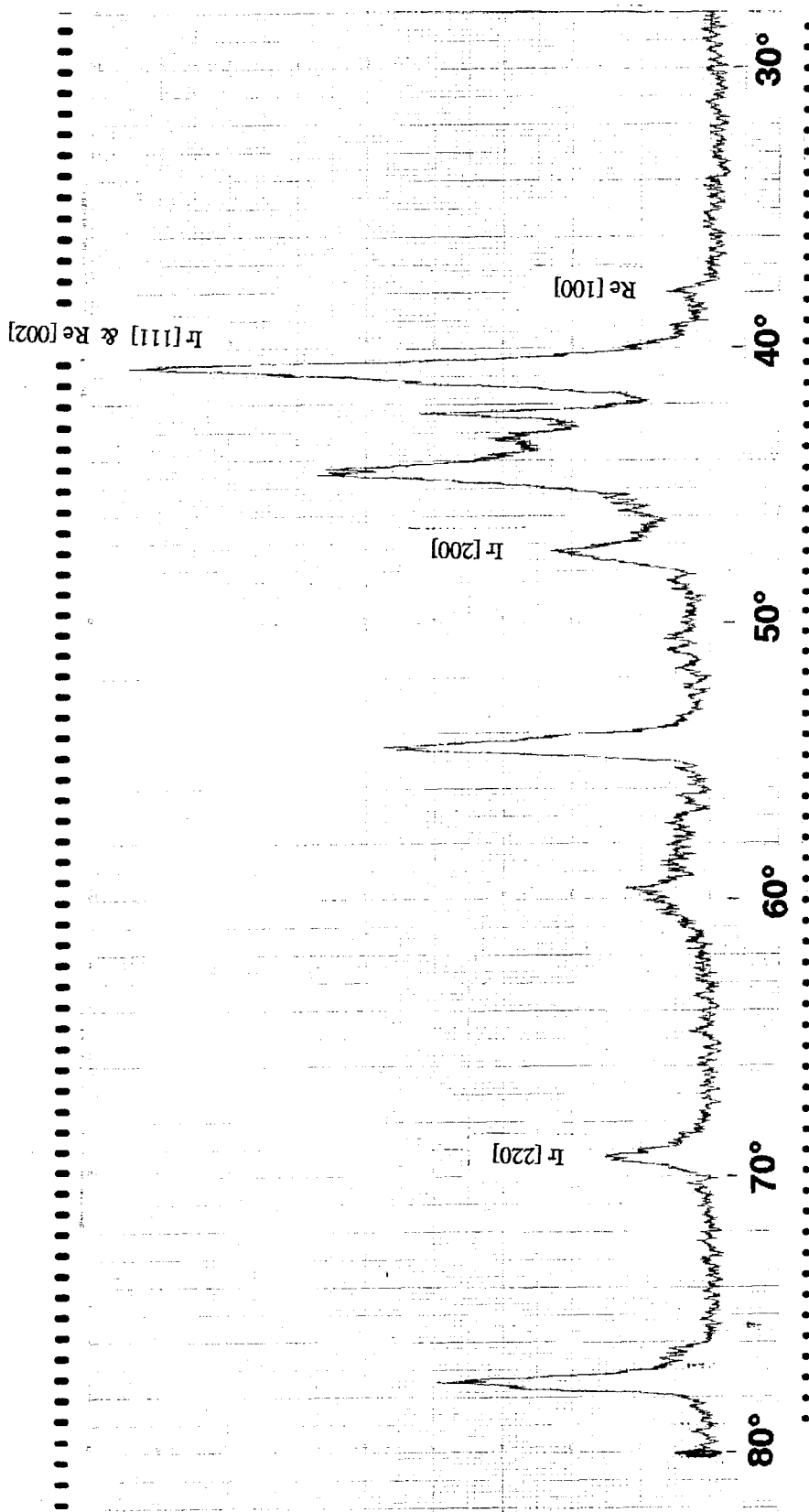


Figure 12

X-ray diffraction pattern for the 90 % Ir / 10 % Re composition on an uncoated graphite substrate.

5.3 Analysis of the coatings following oxidation

A photograph of the oxidized samples is presented in Figure 13. On graphite substrates the compositions 100% Ir and 80% Ir/20% Re exhibited catastrophic oxidation almost immediately. The composition that showed the best oxidation resistance on graphite was 90% Ir/10% Re.

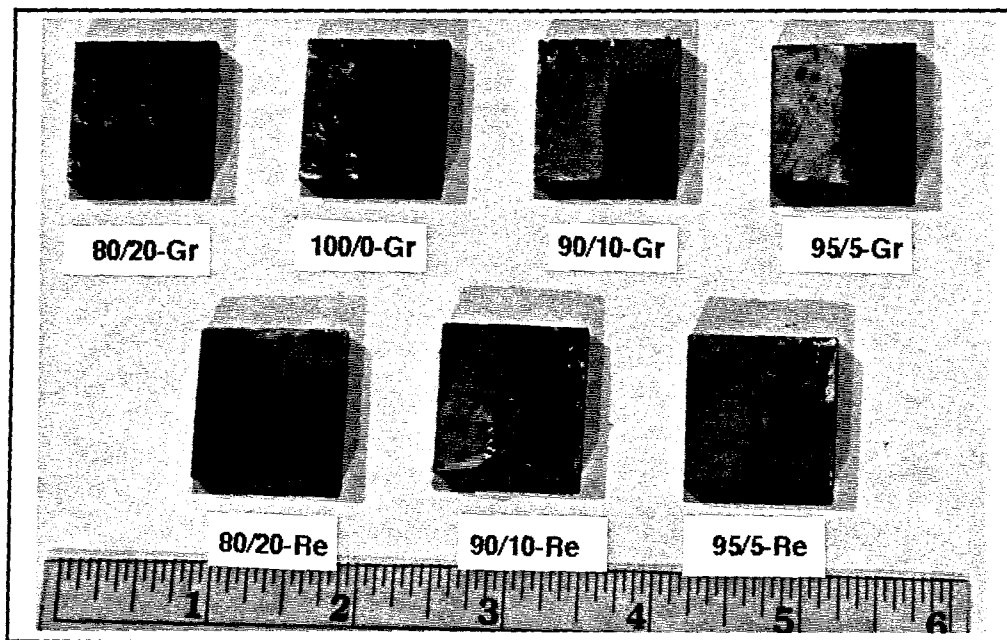


Figure 13. Photograph of the oxidized samples.

On the rhenium coated substrates the film composition 80% Ir/20% Re was completely removed and the underlying rhenium exhibited severe oxidation and cracking, showing a mosaic-like oxidized structure. The codeposited film was intact for the compositions 95% Ir/5% Re and 90% Ir/10% Re. The 90% Ir/10% Re film was less adherent of the two and after mechanically removing this coating the underlying rhenium also exhibited the same mosaic like oxidized structure. The 95% Ir/5% Re film was much more adherent and after mechanical removal the underlying rhenium did not exhibit the mosaic structure and appeared unaffected.

5.4 X-ray Diffraction Analysis of Oxidized Samples

After oxidation testing the samples were again examined by x-ray diffraction. The diffractometer settings were the same as those used for the pre-test scans as listed in Table III. The x-ray diffraction pattern for the sample with 95% Ir / 5% Re composition on rhenium coated substrate is shown in Figure 14. As can be seen, the peaks at 40.6° , 47.3° , and 69.1° 2θ , from the iridium [111], [200], and [220] reflections respectively, are quite sharp and distinct. The rhenium peaks at 42.9° , 37.6° , 67.9° , and 75.2° 2θ corresponding to the [101], [100], and [103] reflections are also sharp and well defined although now of lower intensity than those of the iridium. This indicates an increase in the crystallite size recrystallization of the nano-crystalline deposits. The crystalline size, established from the peak width at half maximum height (PWHMH) technique,⁹ indicates a growth in the average crystallite size from approximately 150Å to 500Å in size during the process of heat treatment.

⁹ B. D. Cullity, "Elements of X-ray Diffraction," Pub Addison and Wesley, 1978.

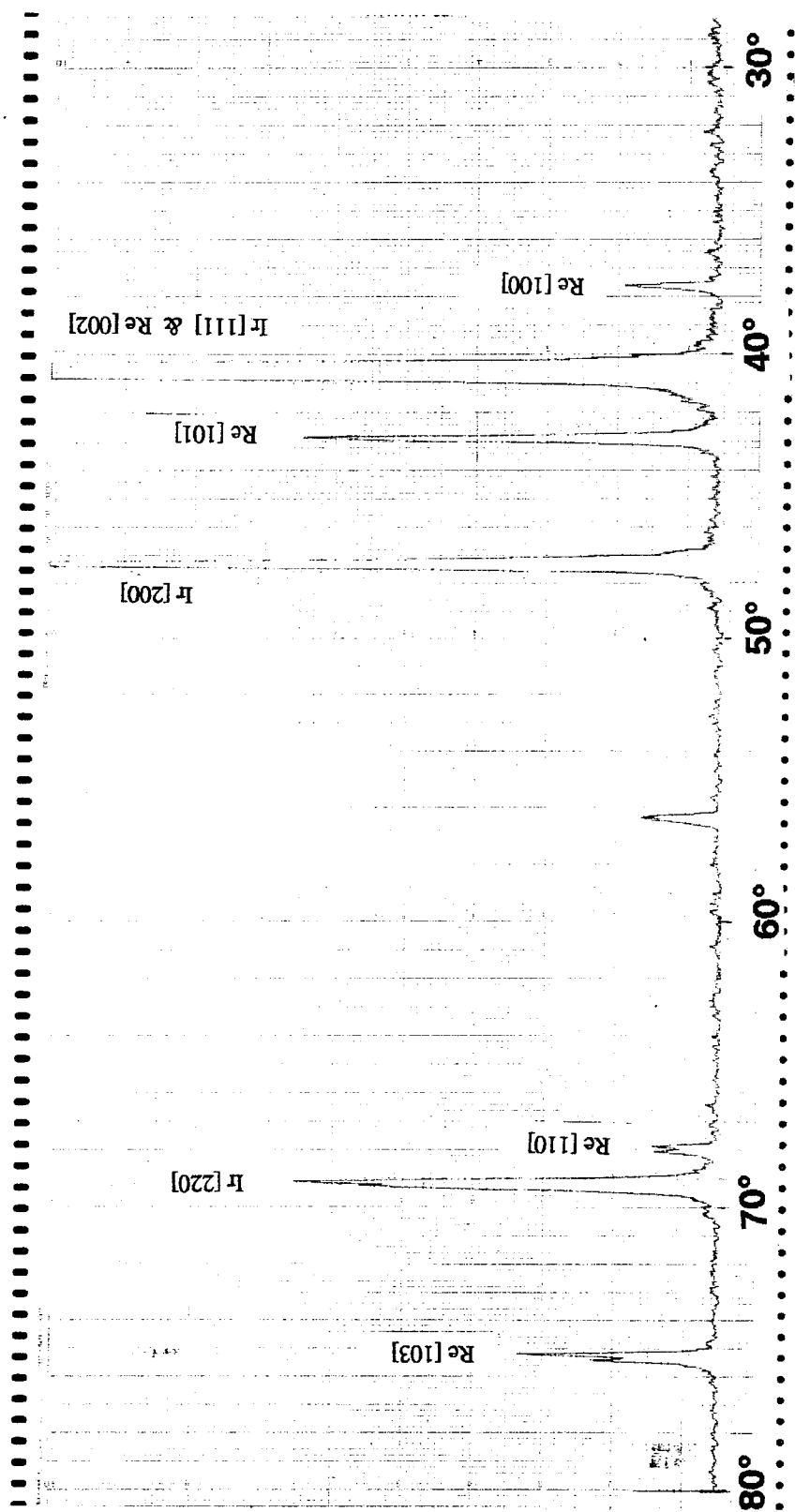


Figure 14.

X-ray diffraction pattern for the 95% Ir / 5% Re composition on rhenium coated substrate after oxidation testing.

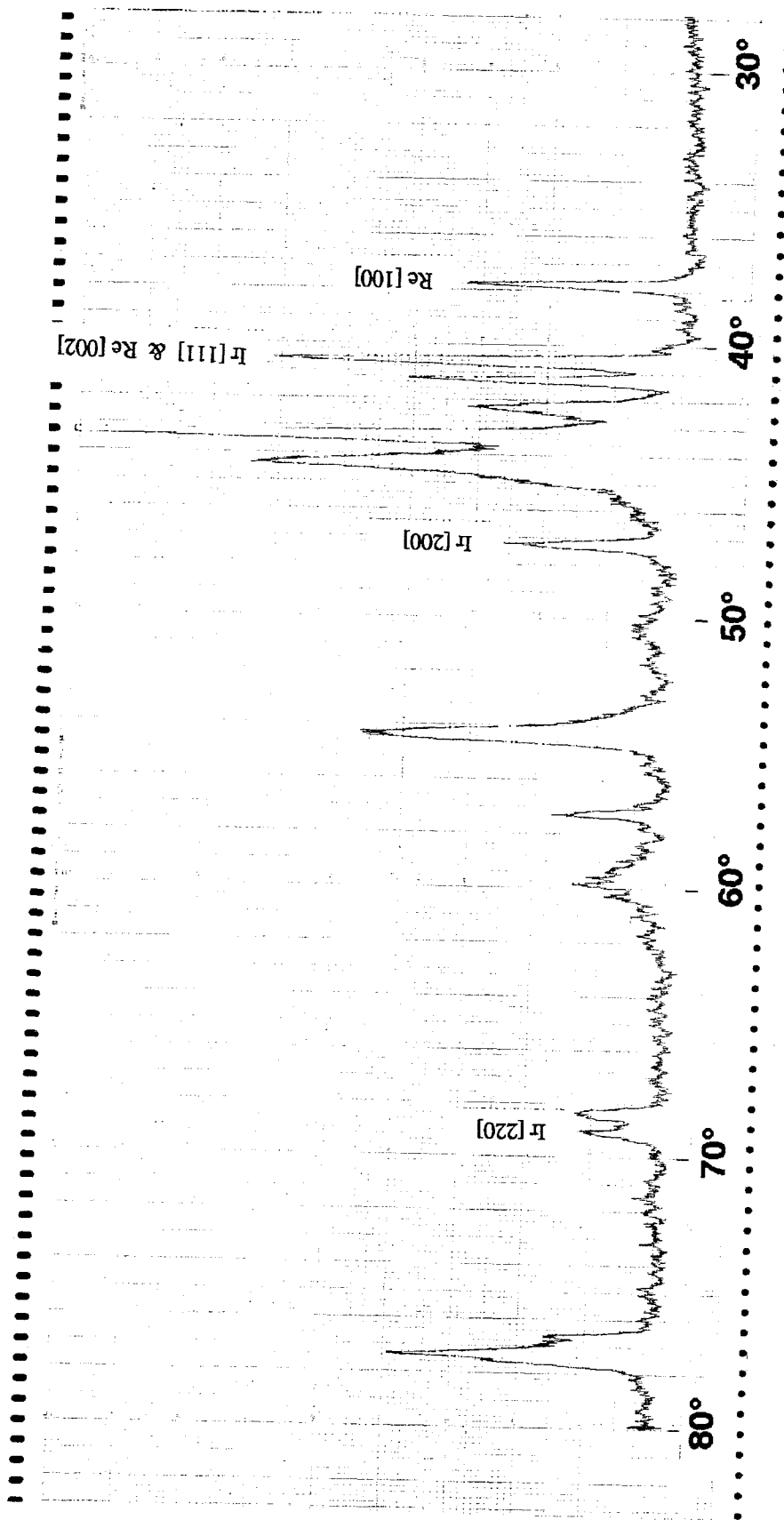


Figure 15

X-ray diffraction pattern for the 90% Ir / 10% Re composition on an uncoated graphite substrate after oxidation testing.

The X-ray diffraction pattern for the 90% Ir / 10% Re coating on an uncoated graphite substrate is shown in Figure 15. As can be seen, the peaks at 40.6° , 47.3° , and $69.1^\circ 2\theta$, from iridium, are quite sharp and distinct. The rhenium peaks corresponding to the [101], [002], [100], and [103] reflections at 42.9° , 40.5° , 37.6° , 67.9° , and $75.2^\circ 2\theta$ are also sharp and well defined although the amount of crystal growth which has taken place is considerably less than with the 95%Ir / 5%Re coating on the Re substrate. An average crystallite size of approximately 200\AA is estimated from the PWHMH technique.

5.5 Fabrication of Fiber Reinforced Ir/Re Thruster

A typical NASA 25lbf thruster designed for evaluating new rocket thruster materials systems was fabricated from braided M30B carbon fibers, infiltrated with an Ir/Re codeposit using the technique developed in this Phase I research. On the basis of the oxidation tests a composition of 95%Ir / 5%Re was chosen as the composition which would provide the best protection for the carbon fiber reinforcement.

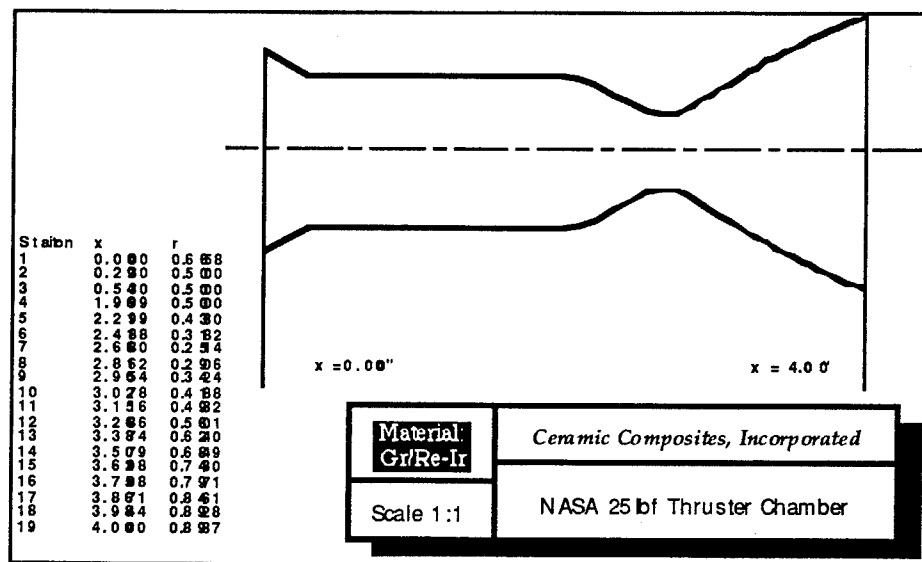


Figure 16 Section of NASA 25lbf thruster

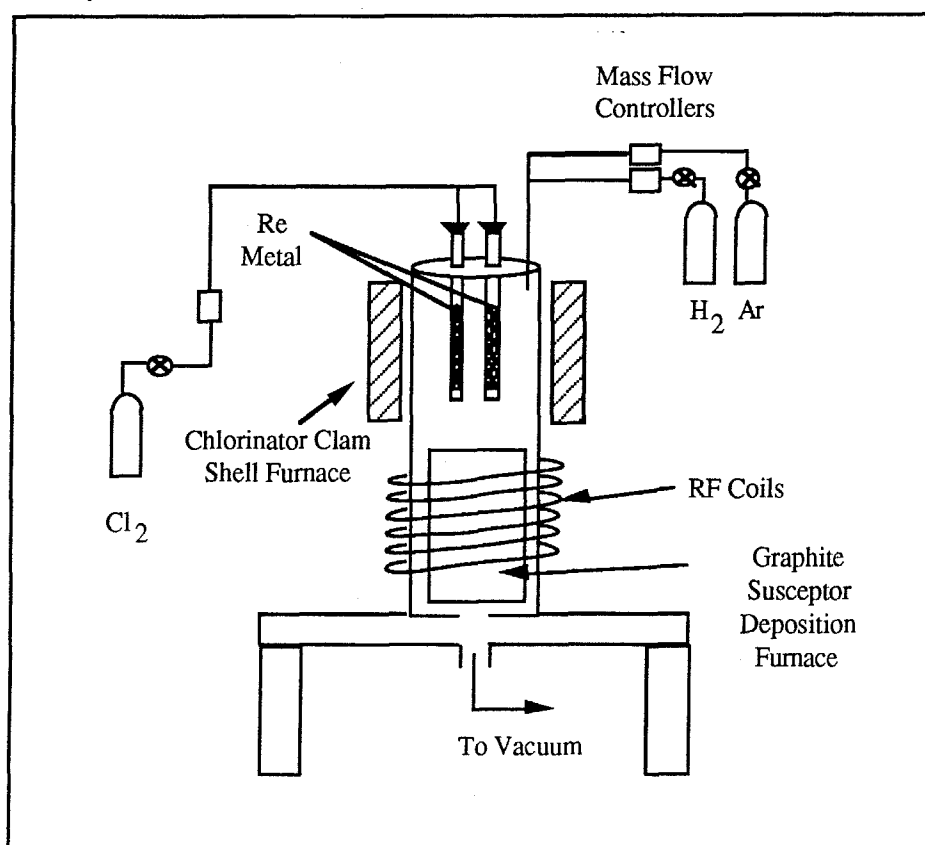
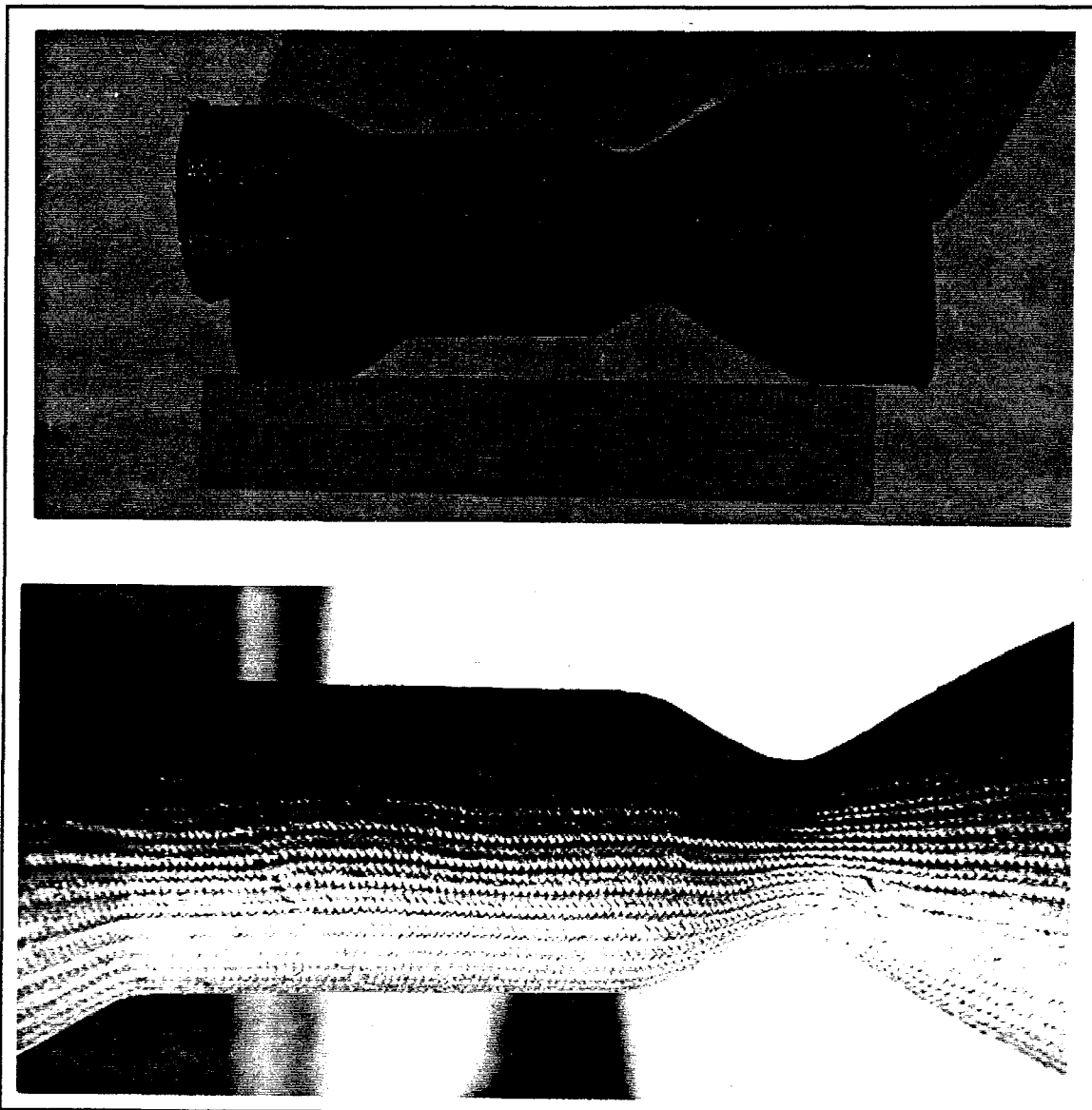


Figure 17 Schematic of the Rhenium Deposition System.

Following discussions with NASA-Lewis regarding design, the graphite (ISO-88) thruster mandrels were ordered from Toyo Tanso, Inc. according to the dimensions shown in Figure 16. After receiving the mandrels, they were shipped to Intec, Inc., where a 30 mil braiding of Mitsui M30B carbon fiber was completed. The braided preform which is shown in Figure 18 was infiltrated from the outside with rhenium for thirty hours. The deposition apparatus is shown schematically in Figure 17. This was followed by twenty-one hours of 90% Ir/10% Re coinfiltration using the low temperature deposition technology developed in this Phase I research. The thruster which was produced is shown in Figure 19. The interior of the thruster was coated in two steps. The reactant flow direction was changed halfway through the deposition run to improve the coating uniformity throughout the length of the thruster.

Following infiltration and coating the density of the thruster was measured using water pycnometry. Measurement of the weight was carried out dry followed by suspension in water. The difference in weight resulted in a direct correlation to the volume of the thruster. The thruster was then boiled in water for 4 hours allowing the open porosity to be filled with water and the saturated weight was measured. The difference between the dry and saturated weights gave a value for the open porosity. The following results were calculated:

Specific Gravity	=	4.013 g/cm ³
Bulk Density	=	2.652 g/cm ³
Open Porosity	=	<u>33.9 %</u>



Figures 18 and 19 Photographs of 25lbf thruster produced, showing the carbon braided mandrel after coating with Re and Ir/Re composition.

Unfortunately, the completed thruster was accidentally damaged during removal of the mandrel while at the CCI facility awaiting shipment to NASA Lewis for testing. The thruster will now be sectioned and characterized through its thickness to assess the infiltration depth and coating uniformity on the carbon fibers by the Re and the Re/Ir codeposit.

6. Technical Feasibility

The results of the Phase I research efforts have directly addressed the issue of the life expectancy in Ir coated Re thrusters by demonstrating that a codeposition of nanocrystalline Ir/Re can be achieved using a novel low temperature CVD Process. Analysis of these coatings deposited using a wide range of process parameters indicate a crystallite size of between 30Å and 1000Å. Oxidation tests have identified the coating compositions

which form the best oxidation barriers on both Re and graphite substrates and characterization of the coating shows that following 30 seconds at 2000 °C the crystallite size of the coating remains approximately 500Å in size. For the Ir/Re codeposits, deposition rates of 0.8 mils/hr have been achieved which although lower than desired is considered reasonable for the Phase I research effort. It is felt that this low temperature CVD technique is generic and can be applied to a wide range of material systems. We also feel that the deposition rates can be considerably improved with further research.

In addition to demonstrating that an oxidation resistant Ir/Re nano-crystalline codeposition can be achieved, we have shown that both Re and the oxidation resistant Ir/Re codeposit can be applied to a carbon fiber preform to fabricate a MMC thruster. This thruster offers a considerable reduction in weight and reduces the manufacturing cost by reducing the consumption of Ir metal. The increased oxidation resistance offered by this nano-crystalline Ir/Re codeposition will impact greatly on the process economics through the manufacture of low density carbon fiber metal matrix composites, as demonstrated by this Phase I research effort.

7. Conclusions and Recommendations

The results of this Phase I research effort have demonstrated that a nano-crystalline codeposit of Ir and Re metal can be achieved by a **novel, low temperature CVD technique**. The deposition parameters have been optimized and the coatings evaluated using an oxyacetylene flame at 2000 °C. The composition and morphology of the most oxidation resistant codeposits have been identified and have been used to coat a carbon fiber thruster, thus demonstrating the ability to significantly impact on the present fabrication economics. The reduction in weight of at least 30% is considered crucial in the lightweighting of on-board spacecraft propulsion systems.

In addition, this low temperature CVD technique is generic in its approach and can be applied to deposit a wide range of nano-crystalline metal coatings. This technique can therefore be applied to directly fabricate coatings of refractory metals such as Ir-Al, La-Ir, which are difficult or impossible to deposit at higher temperatures, or which cannot be deposited due to thermal constraints on the matrix.

In summary the Phase I research produced the following accomplishments;

- Development of a novel low temperature (<425 °C) codeposition CVD process
- Construction and refinement of a two-step organo-chloro metallic codeposition system for Ir-Re alloys
- Deposition of nano-crystalline (30-1000Å) Ir/Re coatings
- Identification of the oxidation resistant compositions: 95%Ir/5%Re on Re and 90%Ir/10%Re on graphite
- Fabrication of an Ir/Re coated Re infiltrated carbon fiber reinforced thruster
- Deposition rates as high as 0.8 mils/hour
- New low temperature CVD process suitable for codeposition of a wide range of refractory materials with unique nano-crystalline structures

It is now important to identify the increase in service life which is offered by this nano-crystalline co-deposit of Ir/Re, over the conventional Ir coated Re thrusters.

This novel low-temperature CVD process is a generic technology and can be used to deposit a wide range of other, difficult to deposit refractory metal coatings such as Ir-Al and Ir-La.

In addition, if this technology is to be applied to the coating of carbon fiber preforms it is important to significantly increase the deposition rate by further investigating changes to the processing parameters.

The ultimate evaluation of this technology needs to be the testing of an MMC thruster fabricated using this nano-crystalline Ir/Re codeposit to coat a carbon fiber preform. An estimate of the wear / oxidation rate can then be made forming a direct comparison with existing Ir coated Re thrusters.

DISTRIBUTION LIST

AUL/LSE Bldg 1405 - 600 Chennault Circle Maxwell AFB, AL 36112-6424	1 cy
DTIC/OCP 8725 John J. Kingman Rd, Suite 0944 Ft Belvoir, VA 22060-6218	2 cys
AFSAA/SAI 1580 Air Force Pentagon Washington, DC 20330-1580	1 cy
PL/SUL Kirtland AFB, NM 87117-5776	2 cys
PL/HO Kirtland AFB, NM 87117-5776	1 cy
Official Record Copy PL/VTS/Lt Bishop Kirtland AFB, NM 87117-5776	2 cys
PL/VT Dr Wick Kirtland AFB, NM 87117-5776	1 cy